

This is an Open Access document downloaded from ORCA, Cardiff University's institutional repository: <https://orca.cardiff.ac.uk/id/eprint/168652/>

This is the author's version of a work that was submitted to / accepted for publication.

Citation for final published version:

Wang, Ke, Xue, Yixun, Zhou, Yue, Li, Zening, Chang, Xinyue and Sun, Hongbin 2024. Distributed coordinated reconfiguration with soft open points for resilience-oriented restoration in integrated electric and heating systems. *Applied Energy* 365, 123207. 10.1016/j.apenergy.2024.123207

Publishers page: <http://dx.doi.org/10.1016/j.apenergy.2024.123207>

Please note:

Changes made as a result of publishing processes such as copy-editing, formatting and page numbers may not be reflected in this version. For the definitive version of this publication, please refer to the published source. You are advised to consult the publisher's version if you wish to cite this paper.

This version is being made available in accordance with publisher policies. See <http://orca.cf.ac.uk/policies.html> for usage policies. Copyright and moral rights for publications made available in ORCA are retained by the copyright holders.



# Distributed Coordinated Reconfiguration with Soft Open Points for Resilience-oriented Restoration in Integrated Electric and Heating Systems

Ke Wang<sup>a,c</sup>, Yixun Xue<sup>a,\*</sup>, Yue Zhou<sup>c</sup>, Zening Li<sup>a</sup>, Xinyue Chang<sup>a</sup>, Hongbin Sun<sup>a,b,\*</sup>

<sup>a</sup> College of Electrical and Power Engineering, Taiyuan University of Technology, Taiyuan 030024, China

<sup>b</sup> Department of Electrical Engineering, Tsinghua University, Beijing 100084, China

<sup>c</sup> Institute of Energy, School of Engineering, Cardiff University, Cardiff CF24 3AA, UK

**Abstract**—As the coupling between power distribution systems (PDSs) and district heating systems (DHSs) becomes tighter, it is critical to develop a coordinated strategy for load restoration in integrated electric and heating systems (IEHSs) after natural catastrophes. Similar to PDS reconfiguration, DHSs can modify network topology by remotely operating the ties and sectionalizing valves. A coordinated reconfiguration with soft open points (SOPs) is proposed in this paper for resilience-oriented restoration in IEHSs, which mitigates the fault propagation during fault isolation and explores the flexibility of network topology variation with SOPs for load restoration. To guarantee the privacy of electric and heating systems, we propose an adaptive alternating direction method of multipliers (ADMM), which divides the original problem into PDS and DHS subproblems. The proposed algorithm can intelligently dispatch SOPs and switches in the PDS sub-problem and valves in the DHS subproblem. Comprehensive case studies are carried out to illustrate the effectiveness of coordinated reconfiguration with SOPs for load restoration and verify the proposed algorithm. When considering coordinated reconfiguration with SOPs under the PDS fault scenario, the resilience metrics value increases by 9.6% compared to only PDS reconfiguration.

**Index Terms**—Integrated electric and heating system, Load restoration, Network reconfiguration, Soft open point, Adaptive alternating direction method of multipliers.

## Nomenclature

### A. Indices and Sets

$t / s$	Index of time/ fault scenario
$T$	Set of the recovery process
$S$	Set of fault scenarios
$T_i / T_r$	Index of fault isolation phase/ restoration phase
$k_k^{CHP}$	Set of CHP units connected to heat station $k$
$k^{pipe} / k^{line}$	Set of lines in PDS/ pipes in DHS
$k^{bus} / k^{node}$	Set of buses in PDS/ nodes in DHS
$k_k^{CHP}$	Set of CHP units
$k^{HB}$	Set of HBs

$k^{HS}$	Set of heat stations
$k_j^{pipe,in} / k_j^{pipe,out}$	Set of pipes flowing from/to node $j$

### B. Parameters

$A_i$	Coefficient of power loss and power generation of SOP $i$ .
$S_i^{SOP}$	Power generation capacity of SOP $i$
$z_{ij,0}$	Boolean variable that represents on/off state of line/pipe $(i, j)$ in normal condition
$s_{ij,0}$	Boolean variable, 1 means the valve/switch on pipe/line $(i, j)$ is in the open position, 0 means pipe/line $(i, j)$ is absence of a valve/switch.
$f_{ij,c}$	Boolean variable that represents whether line/pipe $(i, j)$ is destructed by disaster
$n_s$	Number of root nodes/buses
$n_{ij}$	Number of pipes/lines
$r_{ij} / x_{ij}$	Binary variable that represents whether there is a fault on line/pipe $(i, j)$
$\bar{S}_{ij}$	Transmission limitation of line $(i, j)$
$\underline{u}_j / \bar{u}_j$	Lower/upper square voltage magnitude of bus $j$ .
$\underline{p}_j^{DG} / \bar{p}_j^{DG}$	Lower/upper power output of DG $j$
$\underline{p}_j^{CHP} / \bar{p}_j^{CHP}$	Lower/upper power output of CHP unit $j$
$\underline{v}_j / \bar{v}_j$	Lower/upper coefficient of power and heat generation of CHP unit $j$
$\gamma_j$	Coefficient between heat generation and fuel consumption of HB $j$
$\bar{h}_{ij}^P$	Transmission limitation of pipe $(i, j)$
$a_j / b_j$	Weight of electric and heat load $j$
$\Delta T_i / \Delta T_r$	Fault isolation duration/ restoration duration

✧ The short version of the paper was presented at CUE 2023, Matsue, Japan, Sept. 2-5, 2023. This paper is a substantial extension of the short version of the conference paper.

\*Corresponding authors.

E-mail address: WangK50@cardiff.ac.uk (K. Wang), xueyixun@tyut.edu.cn (Y. Xue), ZhouY68@cardiff.ac.uk (Y. Zhou), lizening@tyut.edu.cn (Z. Li), changxy16@foxmail.com (X. Chang), shb@tsinghua.edu.cn (H. Sun)

### C. Variables

$p_{i,s,t}^{SOP} / q_{i,s,t}^{SOP}$	Active/reactive power generation of SOP $i$ at period $t$
$p_{i,s,t}^{SOP,Loss} / q_{i,s,t}^{SOP,Loss}$	Active/reactive power loss of SOP $i$ at period $t$
$z_{ij,s,t}$	Boolean variable that represents the on/off state of line/pipe $(i,j)$ at period $t$
$\chi_{i,s,t}$	Boolean variable that represents the faulty/unfaulty state of bus $i$ at period $t$
$a_{ij,s,t}$	Boolean variable that represents virtual power flow between buses $i$ and $j$ at period $t$
$d_{j,s,t}$	Boolean variable that represents virtual power demand at bus $j$ at period $t$
$l_{ij,s,t}$	Square of current of line $(i,j)$ at period $t$
$p_{j,s,t} / q_{j,s,t}$	Power injection of bus $i$ at period $t$
$p_{ij,s,t} / q_{ij,s,t}$	Power flow from bus $i$ to bus $j$ at period $t$
$p_{j,s,t}^{DG} / q_{j,s,t}^{DG}$	Power output of DG $j$ at period $t$
$p_{j,s,t}^{CHP} / q_{j,s,t}^{CHP}$	Power output of CHP unit $j$ at period $t$
$p_{j,s,t}^L / q_{j,s,t}^L$	Electric load of bus $j$ at period $t$
$p_{j,s,t}^{Loss} / q_{j,s,t}^{Loss}$	Electric Load loss of bus $j$ at period $t$
$u_{i,s,t}$	Square of bus voltage at period $t$
$h_{j,s,t}^{CHP}$	Heat output of CHP unit $j$ at period $t$
$h_{j,s,t}^{HB}$	Heat output of HB $j$ at period $t$
$f_{j,s,t}^{HB}$	Fuel consumption of HB $j$ at period $t$
$h_{k,s,t}^{HS}$	Heat generation of heat station $k$ at period $t$
$h_{ij,s,t}^{P,start} / h_{ij,s,t}^{P,end}$	Inlet/outlet thermal power of pipe $(i,j)$ at period $t$
$h_{ij,s,t}^{loss}$	Loss thermal power of pipe $(i,j)$ at period $t$
$p_t^{Nloss}$	Power loss of bus $j$ at period $t$

## 1. Introduction

In recent years, climate change has increased the occurrence and intensity of natural disasters, such as snowstorms, earthquakes, and ice disasters [1]-[2]. Critical energy infrastructures, such as power lines and heating pipelines, are vulnerable to disasters, resulting in significant destruction. Infrastructure vulnerability can cause significant disruptions in the energy supply [3]. The Texas frost in 2021 left almost 4.5 million consumers without power at peak, in which economic

damages from missed power production were \$130 billion [4]. The Jilin ice disaster in 2020 caused power transmission lines to break, which in turn compelled the Changchun thermal power plant unit to halt operations, and more than 300 million people faced power and heating outages.

As the aforementioned concerns become more prevalent, resilience-oriented load restoration of energy systems has gained prominence after natural catastrophes, particularly in power systems. Load restoration after disasters commonly includes fault isolation and service restoration stages [5]. In the fault isolation stage, fault areas are identified precisely [6]. Ref [7] proposed a novel model to determine faulted zones with loops, which considered the change of network topology in the power system. In the short-term restoration stage, fast-responding flexible resources are invoked to ensure timely power restoration, such as network reconfiguration [8].

Other researchers have investigated further methods for restoring integrated energy systems [9]. Ref [10] proposed a restoration strategy for regional-level integrated energy systems considering the operation flexibility of district-level integrated energy systems. Ref [11] developed a load restoration strategy for integrated power and natural gas systems, which considered complicated influential relations between subsystems. Ref [12] proposed a coordinated dispatch strategy for the repair crews to ensure energy supply for important loads in integrated power and natural gas systems. However, previous studies have primarily concentrated on power systems or integrated power and natural gas systems.

The growing deployment of combined heat and power (CHP) units has heightened the interdependence between power distribution systems (PDSs) and district heating systems (DHSs). The installed capacity of CHP units in China is 550 million kW, representing 42% of the total installed capacity of thermal power and fulfilling over 67% of the national heating demands [13]. The intricate coupling properties between PDSs and DHSs have presented significant hurdles for resilience-oriented load restoration in integrated electric and heating systems (IEHSs) [14]: i) during the fault isolation stage, the occurrence of faults in the PDS/DHS may transfer to the other system through coupling components, causing extra load loss [15]. For instance, improper switching operation in PDS might influence the heat outputs of the CHP unit, resulting in the unnecessary shedding of heat loads; ii) during the short-term restoration stage, the operational flexibility of the IEHS, such as the fast adjustment capability of the CHP unit, cannot be fully exploited when subsystems operate independently unless they are coordinated with the CHP power generation in PDS. Therefore, it is necessary to employ a collaborative service restoration method for fast service restoration in IEHSs.

Soft open points (SOPs) are electronic devices that regulate active power flow and voltage, while also compensating for reactive power, which is an essential instrument for PDS restoration [16]. Ref [17] introduced a restoration strategy considering the structure and capability of SOPs on service recovery in power systems. However, SOPs have not been considered in the IEHS collaborative recovery procedure.

Compared with traditional switches, SOPs could provide additional power to restore lost electric loads and restructure the optimal energy supply of coupling units when connected with them, resulting in the reduction of fault propagation and total load loss in IEHSs after natural disasters.

The DHS reconfiguration is a major method for improving load restoration. Similar to PDS reconfiguration, DHS can modify network topology by remoting the actuation of ties and sectionalizing valves [18]. Following the DHS design code, both ties and sectionalizing valves can be turned on/off to restore heat supply. Sectionalizing valves are installed to isolate pipeline sections during emergencies, such as pipeline leaks. Tie valves are engineered to reallocate heating loads among heat sources after disasters, curtailing needless load shedding in IEHS. More importantly, the DHS network structure can be altered to function with the switches in the PDS to decrease the amount of excessive load shedding and prevent further fault propagation among subsystems. Essentially, coordinated reconfiguration of both subsystems can explore the adaptability of time-varying topology for short-term restoration.

Besides, the above studies have been carried out in a centralized way, assuming that a central operator monitors the electric and heating subsystems, ignoring the barriers in information exchange and management between the electric and heating systems [19]-[20]. The two sub-systems may not be consistently managed by a single central operator. Furthermore, the centralized method fails to protect the privacy security of each subsystem due to the massive amount of private data exchanged. The conventional centralized optimal method may not be applicable and a distributed approach is required to realize the synergistic operation of IEHS.

Accordingly, this research puts forth distributed coordinated reconfiguration with SOPs for resilience-oriented restoration. The contributions are summed up as follows:

- 1) SOPs have been first brought into focus in the collaborative recovery process of IEHSs, which can provide extra power to lost electric loads and adjust the optimal energy supply of coupling units, which can mitigate fault propagation and reduce total load loss in IEHSs after natural disasters.
  - 2) Coordinated reconfiguration in the proposed coordinated service restoration model (CSRSM) is provided to explore the flexibility of time-varying network topology for fast service restoration. The DHS network structure is adjusted in collaboration with the PDS switching operation, which can prevent excessive load shedding and halt tremendous fault propagations in respective networks.
  - 3) To guarantee the privacy security of electric and heating systems, we propose an adaptive alternating direction method of multipliers (ADMM). The original coordinated service restoration problem is divided into PDS and DHS sub-problems, which can intelligently dispatch SOPs in the PDS sub-problem and network reconfiguration in the DHS sub-problem with the least transmitted information. Also, the step size is modified in each iteration to improve convergence performance.
- The following sections are structured as follows: Section 2

describes a typical IEHS and illustrates the reciprocal influences between subsystems during the whole recovery process. In Section 3, CSRSM is formulated, investigating the fault propagation between subsystems, and the control and operation of SOPs for service restoration. In Section 4, an adaptive ADMM is proposed to guarantee the privacy of electric and heating systems. In Section 5, the results from the P33H14 and P118H32 systems are discussed. In Section 6, the conclusions and recommendations for further research are presented.

## 2. Problem Description

Fig.1 shows the structure of a typical IEHS, which is made up of PDS and DHS. The CHP units, being the primary heat source in DHS and the main generators in PDS, bolster the linkage between these two systems. SOPs are electronic devices that are installed in place of regular open points in PDS, which can provide additional power supply for lost loads. Furthermore, PDS and DHS reconfigurations are coordinated by valve operations in DHS in tandem with switching operations in PDS.

To demonstrate the reciprocal influences of the subsystems and ensure energy supply to critical loads, this study proposes coordinated reconfiguration with SOPs for resilience-oriented restoration, which incorporates fault isolation and load restoration stages. In the fault isolation stage, faulty regions are accurately isolated by the operations of SOPs, switches, and valves. In the restoration stage, the DHS network structure is adjusted in collaboration with SOPs and switch operation in PDS, which can prevent excessive load shedding and halt tremendous fault propagations in respective networks.

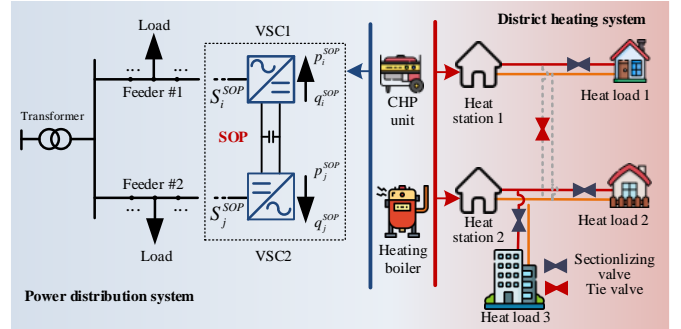


Fig.1. A typical IEHS with SOPs

## 3. Formulation of CSRSM

A coordinated service restoration model encompassing fault isolation and restoration is developed in this section, primarily employed for fast service restoration. The model illustrates the propagation between subsystems during the isolation stage and explores the impact of coordinated reconfiguration with SOPs on load restoration.

### 3.1. SOP Constraints

Back-to-back voltage-source converters (VSC) are used in SOPs, and two control modes have been designed for SOP operation, i.e.,  $V_{ac}Q-V_{acf}$  and  $V_{ac}Q-PQ$  control modes. In the analysis of supply restoration of PDS,  $V_{ac}Q-V_{acf}$  control mode

will be initiated [21]. SOPs will operate in  $V_{ac}f$  control mode to supply power to lost loads on the faulty side and operate in  $V_{dc}Q$  control mode on the unfaulty side [22]. The SOP constraints are formulated as follows:

$$p_{i,s,t}^{SOP} + p_{j,s,t}^{SOP} + p_{i,s,t}^{SOP,Loss} + p_{j,s,t}^{SOP,Loss} = 0, \quad (1)$$

$$\forall t \in T, \forall s \in S,$$

$$p_{i,s,t}^{SOP,Loss} = A_i \left\| p_{i,s,t}^{SOP} \quad q_{i,s,t}^{SOP} \right\|_2, \forall t \in T, \forall s \in S, \quad (2)$$

$$p_{j,s,t}^{SOP,Loss} = A_j \left\| p_{j,s,t}^{SOP} \quad q_{j,s,t}^{SOP} \right\|_2, \forall t \in T, \forall s \in S, \quad (3)$$

$$\left\| p_{i,s,t}^{SOP} \quad q_{i,s,t}^{SOP} \right\|_2 \leq S_i^{SOP}, \forall t \in T, \forall s \in S, \quad (4)$$

$$\left\| p_{j,s,t}^{SOP} \quad q_{j,s,t}^{SOP} \right\|_2 \leq S_j^{SOP}, \forall t \in T, \forall s \in S, \quad (5)$$

$$u_{j,s,t}^{SOP} \geq u_0^2, \forall t \in T, \forall s \in S, \quad (6)$$

Constraint (1) demonstrates that the power injections and power losses of connected buses with SOP should maintain balance; Constraints (2)-(3) illustrate the power loss of SOP at connected buses  $i$  and  $j$ , primarily through semiconductor switch conduction losses, switching, and capacitor losses. Constraints (4)-(5) illustrate the power limitation of SOP at connected buses  $i$  and  $j$ . Constraint (6) illustrates voltage magnitude constraint on the non-faulted side of SOP.

### 3.2. Topological Constraints

#### 3.2.1 Fault Isolation Constraints

The fault propagation is described by the fault isolation model, which is designed to precisely identify faulty region. It is expressed as follows:

$$(1 - f_{ij,s}) (z_{ij,0} - s_{ij,0}) \leq z_{ij,s,t} \leq (1 - f_{ij,s}) z_{ij,0}, \quad (7)$$

$$\forall (i,j) \in k^{pipe} \cup k^{line}, \forall t \in T_i, \forall s \in S, \quad (7)$$

$$\chi_{i,s,t} + 1 \geq f_{ij,s} (1 - s_{ij,0}) + z_{ij,0}, \quad (8)$$

$$\forall (i,j) \in k^{pipe} \cup k^{line}, \forall t \in T_i, \forall s \in S, \quad (8)$$

$$\chi_{j,s,t} + 1 \geq f_{ij,s} (1 - s_{ij,0}) + z_{ij,0}, \quad (9)$$

$$\forall (i,j) \in k^{pipe} \cup k^{line}, \forall t \in T_i, \forall s \in S, \quad (9)$$

$$\chi_{j,s,t} - \chi_{i,s,t} \geq z_{ij,s,t} - 1, \quad (10)$$

$$\forall (i,j) \in k^{pipe} \cup k^{line}, \forall t \in T_i, \forall s \in S, \quad (10)$$

$$\chi_{i,s,t} - \chi_{j,s,t} \geq z_{ij,s,t} - 1, \quad (11)$$

$$\forall (i,j) \in k^{pipe} \cup k^{line}, \forall t \in T_i, \forall s \in S, \quad (11)$$

$$\chi_{g,s,t} = \chi_{h,s,t}, \quad (12)$$

$$\forall g \in k_{i,h}^{CHP}, h \in k_{i,e}^{CHP}, \forall t \in T_i, \forall s \in S, \quad (12)$$

Constraint (7) illustrates that the switches/valves equipped on non-faulty pipe/line  $(i,j)$  could be operated to promptly isolate faults. Constraints (8)-(9) demonstrate that if the switch/valve is equipped on a damaged pipe/line  $(i,j)$ , the connected nodes/buses  $i$  and  $j$  will be included in the non-faulty region. Constraints (10)-(11) illustrate that the nodes/buses  $i$  and  $j$  of a closed pipe/line  $(i,j)$  will be divided in the same region. Constraint (12) indicates that when the CHP

unit  $i$  has belonged to the faulty region within DHS analysis, it would belong to the faulty region within PDS analysis.

#### 3.2.2 Service Restoration Constraints

In the restoration stage, SOPs, switches, and valves will be utilized to restore lost loads in non-faulty regions defined in the last stage. The subsequent topological constraints are formulated:

$$(1 - f_{ij,s}) (z_{ij,t-1} - s_{ij,0}) \leq z_{ij,s,t} \leq (1 - f_{ij,s}) (z_{ij,t-1} + s_{ij,0}), \quad (13)$$

$$\forall (i,j) \in k^{pipe} \cup k^{line}, \forall t \in T_r, \forall s \in S,$$

$$\sum_{i:j \rightarrow i} a_{ji,s,t} + d_{j,s,t} = \sum_{h:h \rightarrow j} a_{hj,s,t}, \quad (14)$$

$$\forall i \in n_{ij} \setminus n_s, \forall t \in T_r, \forall s \in S,$$

$$|a_{ji,s,t}| \leq z_{ij,s,t} n_{ij}, \quad (15)$$

$$\forall (i,j) \in k^{pipe} \cup k^{line}, \forall t \in T_r, \forall s \in S,$$

$$\sum_{(i,j) \in k^{pipe} \cup k^{line}} z_{ij,s,t} = n_{ij} - n_s, \forall t \in T_r, \forall s \in S, \quad (16)$$

$$\chi_{j,s,t-1} - \chi_{i,s,t-1} \geq z_{ij,s,t} - 1, \quad (17)$$

$$\forall (i,j) \in k^{pipe} \cup k^{line}, \forall t \in T_r, \forall s \in S,$$

$$\chi_{i,s,t-1} - \chi_{j,s,t-1} \geq z_{ij,s,t} - 1, \quad (18)$$

$$\forall (i,j) \in k^{pipe} \cup k^{line}, \forall t \in T_r, \forall s \in S,$$

Constraint (13) illustrates that the switch/valve on non-faulty pipes/lines  $(i,j)$  can be operated for network reconfiguration of PDS and DHS. When  $f_{ij,s} = 0$ ,  $s_{ij,0} = 1$ , the operation status of pipes/line  $(i,j)$ , denoted as 0 or 1, can be adjusted, which is essential for the dynamic reconfiguration of both PDS and DHS. Constraints (14)-(16) demonstrate the condition for radial topology in PDS and DHS [23]. Here the root node in PDS includes power sources and nodes connected to SOPs on the faulty side. Constraints (17)-(18) illustrate reconnecting non-faulty buses/nodes to the faulty ones that are separated in the previous stage is not permitted.

### 3.3. Operation Constraints

#### 3.3.1 PDS Operation Constraints

The PDS operation model for the coordinated service restoration problem is formulated as a mixed-integer second-order cone programming (MISOCP) problem, which is shown as follows

$$p_{j,s,t} = \sum_{s \in \delta(j)} p_{js,s,t} - \sum_{i \in \pi(j)} (p_{ij,s,t} - r_{ij} l_{ij,s,t}), \quad (19)$$

$$\forall j \in k^{bus}, \forall t \in T, \forall s \in S,$$

$$q_{j,s,t} = \sum_{s \in \delta(j)} q_{js,s,t} - \sum_{i \in \pi(j)} (q_{ij,s,t} - x_{ij} l_{ij,s,t}), \quad (20)$$

$$\forall j \in k^{bus}, \forall t \in T, \forall s \in S,$$

$$\begin{aligned}
p_{j,s,t} &= p_{j,s,t}^{DG} + p_{j,s,t}^{CHP} + p_{j,s,t}^{SOP} - (p_{j,s,t}^L - p_{j,s,t}^{Loss}), \\
\forall j \in k^{bus}, \forall t \in T, \forall s \in S, \\
q_{j,s,t} &= q_{j,s,t}^{DG} + q_{j,s,t}^{CHP} + q_{j,s,t}^{SOP} - (q_{j,s,t}^L - q_{j,s,t}^{Loss}), \\
\forall j \in k^{bus}, \forall t \in T, \forall s \in S,
\end{aligned} \quad (21)$$

Constraints (19)-(20) illustrate the power balance at bus  $j$ . Constraints (21)-(22) illustrate the injected power at bus  $j$  considering the power injection of SOP.

$$\|2p_{ij,s,t} - 2q_{ij,s,t} - l_{ij,s,t} - u_{i,s,t}\|_2 \leq l_{ij,s,t} + u_{i,s,t}, \quad (23)$$

$$\begin{aligned}
\forall j \in k^{bus}, \forall t \in T, \forall s \in S, \\
-z_{ij,s,t} \bar{S}_{ij} \leq p_{ij,s,t} \leq z_{ij,s,t} \bar{S}_{ij}, \\
\forall (i,j) \in k^{line}, \forall t \in T, \forall s \in S,
\end{aligned} \quad (24)$$

$$\begin{aligned}
-z_{ij,s,t} \bar{S}_{ij} \leq q_{ij,s,t} \leq z_{ij,s,t} \bar{S}_{ij}, \\
\forall (i,j) \in k^{line}, \forall t \in T, \forall s \in S,
\end{aligned} \quad (25)$$

Constraint (23) illustrates the relaxed branch power flow equation of line  $(i,j)$ . Constraints (24)-(25) illustrate the transmission limitation of line  $(i,j)$ .

$$\begin{aligned}
u_{i,s,t} - u_{j,s,t} - 2(r_{ij} p_{ij,s,t} + x_{ij} q_{ij,s,t}) + (r_{ij}^2 + x_{ij}^2) l_{ij,s,t} \\
\leq (1 - z_{ij,s,t}) M, \forall (i,j) \in k^{line}, \forall t \in T, \forall s \in S,
\end{aligned} \quad (26)$$

$$\begin{aligned}
u_{i,s,t} - u_{j,s,t} - 2(r_{ij} p_{ij,s,t} + x_{ij} q_{ij,s,t}) + (r_{ij}^2 + x_{ij}^2) l_{ij,s,t} \\
\geq (1 - z_{ij,s,t}) M, \forall (i,j) \in k^{line}, \forall t \in T, \forall s \in S,
\end{aligned} \quad (27)$$

$$\bar{u}_j \leq u_{j,s,t} \leq \bar{u}_j, \forall j \in k^{bus}, \forall t \in T, \forall s \in S, \quad (28)$$

Constraints (26)-(28) formulate the relationship between node voltage values at connected buses  $i$  and  $j$  illustrate that node voltage values at separated buses  $i$  and  $j$  cannot be influenced each other.

$$\begin{aligned}
(1 - \chi_{j,s,t}) p_j^{CHP} \leq p_{j,s,t}^{CHP} \leq (1 - \chi_{j,s,t}) \bar{p}_j^{CHP}, \\
\forall j \in k^{CHP}, \forall t \in T, \forall s \in S,
\end{aligned} \quad (29)$$

$$\begin{aligned}
(1 - \chi_{j,s,t}) q_j^{CHP} \leq q_{j,s,t}^{CHP} \leq (1 - \chi_{j,s,t}) \bar{q}_j^{CHP}, \\
\forall j \in k^{CHP}, \forall t \in T, \forall s \in S,
\end{aligned} \quad (30)$$

$$\begin{aligned}
(1 - \chi_{j,s,t}) p_j^{DG} \leq p_{j,s,t}^{DG} \leq (1 - \chi_{j,s,t}) \bar{p}_j^{DG}, \\
\forall j \in k^{DG}, \forall t \in T, \forall s \in S,
\end{aligned} \quad (31)$$

$$\begin{aligned}
(1 - \chi_{j,s,t}) q_j^{DG} \leq q_{j,s,t}^{DG} \leq (1 - \chi_{j,s,t}) \bar{q}_j^{DG}, \\
\forall j \in k^{DG}, \forall t \in T, \forall s \in S,
\end{aligned} \quad (32)$$

Constraints (29)-(32) illustrate the power source generation, including the CHP unit  $j$  and DG  $j$ , in the faulty/non-faulty region. For example, if the CHP unit  $j$  is shut down in the faulty region, its power generation will be reduced to zero. The power output of the CHP unit  $j$  in the non-faulty region is constrained within upper and lower limitations.

$$\chi_{j,s,t} p_j^L \leq p_{j,s,t}^{Loss} \leq p_j^L, \forall j \in k^{bus}, \forall t \in T, \forall s \in S, \quad (33)$$

$$\chi_{j,s,t} q_j^L \leq q_{j,s,t}^{Loss} \leq q_j^L, \forall j \in k^{bus}, \forall t \in T, \forall s \in S, \quad (34)$$

Constraints (33)-(34) illustrate that electric loads in faulty regions will be completely disconnected due to unit shutdown, while partially lost to maintain energy balance in non-faulty regions.

### 3.3.2 DHS Operation Constraints

The exact DHS operation model poses challenges due to it being a mixed-integer nonlinear programming problem, which becomes troublesome especially when applied in CSRM [24]. Therefore, we use an energy flow (EF) model that decouples the thermal power from the mass flow rate and the temperature to avoid the abovementioned problem. The EF model is well-suited for fast load restoration, especially when involving the DHS restructuring, as it maintains a balance between accuracy and computation speed [25]-[26].

$$\underline{v}_j h_{j,s,t}^{CHP} \leq p_{j,s,t}^{CHP} \leq \bar{v}_j h_{j,s,t}^{CHP}, \forall j \in k^{CHP}, \forall t \in T, \forall s \in S, \quad (35)$$

$$h_{j,s,t}^{HB} = \gamma_j f_{j,s,t}^{HB}, \forall j \in k^{HB}, \forall t \in T, \forall s \in S, \quad (36)$$

$$\sum_{j \in k_j^{CHP}} h_{j,s,t}^{CHP} + \sum_{j \in k_j^{HB}} h_{j,s,t}^{HB} = h_{k,s,t}^{HS}, \forall k \in k^{HS}, \forall t \in T, \forall s \in S, \quad (37)$$

$$\sum_{(j,s) \in k_j^{pipe,out}} h_{j,s,t}^{P,start} + \sum_{k \in k_j^{HS}} h_{k,s,t}^{HS} = h_{j,s}^L - h_{j,s}^{Loss} + \sum_{(i,j) \in k_j^{pipe,in}} h_{i,s,t}^{P,end}, \quad (38)$$

$$\forall j \in k^{nd}, \forall t \in T, \forall s \in S,$$

Constraint (35) demonstrates the relation between power and heat generation of CHP unit  $j$ . Constraint (36) illustrates the relationship between heat output and fuel consumption of the heating boiler (HB)  $j$ . Constraint (37) illustrates that the generated heat at the station  $k$  includes those of the installed CHP unit, and HB. Constraint (38) illustrates the energy balance of node  $j$ .

$$h_{i,j,s,t}^{P,end} = h_{i,j,s,t}^{P,start} - h_{i,j,s,t}^{loss}, \forall (i,j) \in k^{pipe}, \forall t \in T, \forall s \in S, \quad (39)$$

$$0 \leq |h_{i,j,s,t}^{P,start}| \leq z_{ij,s,t} \bar{h}_{ij}, \forall (i,j) \in k^{pipe}, \forall t \in T, \forall s \in S, \quad (40)$$

$$0 \leq |h_{i,j,s,t}^{P,end}| \leq z_{ij,s,t} \bar{h}_{ij}, \forall (i,j) \in k^{pipe}, \forall t \in T, \forall s \in S, \quad (41)$$

Constraint (39) illustrates the heat loss between the outlet and the inlet of pipe  $(i,j)$ . Constraints (40)-(41) guarantee that the energy flow in the pipe can vary after reconfiguration.

$$(1 - \chi_{j,s,t}) \underline{h}_j^{CHP} \leq h_{j,t}^{CHP} \leq (1 - \chi_{j,s,t}) \bar{h}_j^{CHP}, \quad (42)$$

$$\forall j \in k^{CHP}, \forall t \in T, \forall s \in S,$$

$$(1 - \chi_{j,s,t}) \underline{h}_j^{HB} \leq h_{j,s,t}^{HB} \leq (1 - \chi_{j,s,t}) \bar{h}_j^{HB}, \quad (43)$$

$$\forall j \in k^{HB}, \forall t \in T, \forall s \in S,$$

Constraints (42)-(43) illustrates that the shutdown of heat sources in the faulty region, such as the CHP unit  $j$ , and HB  $j$ , will result in the heat outputs being zero. Meanwhile, constraints (42)-(43) illustrate the heat output limit of heat sources in the non-faulty region.

$$\chi_{j,s,t} h_j^L \leq h_{j,s,t}^{Loss} \leq h_j^L, \forall j \in k^{nd}, \forall t \in T, \forall s \in S, \quad (44)$$

Constraint (44) illustrates that the heat loads would be fully dissipated in the faulty areas, while partially lost for energy balance in the non-faulty areas.

### 3.4. Objective and Resilience Metrics

The objective in (45) is to maximize the load restoration in the whole recovery process to guarantee that critical electric and heating loads obtain longer energy supplies. The second item is the network loss penalty to ensure the accuracy of the CSRMM after second-order cone relaxation and  $\sigma$  should be small enough. The resilience metrics in (46) quantify the ratio of total load losses in PDS and DHS throughout the entire restoration process, which serves as an indicator of the load recovery level during the process.

$$\min f = \sum_{s \in \mathcal{S}} p_s \left[ \Delta T_i \left( \sum_{j \in k^{bus}} a_j p_{j,s,t}^{Loss} + \sum_{j \in k^{nd}} b_j h_{j,s,t}^{Loss} \right) + \Delta T_r \left( \sum_{j \in k^{bus}} a_j p_{j,s,t}^{Loss} + \sum_{j \in k^{nd}} b_j h_{j,s,t}^{Loss} \right) \right] + \sigma \sum_{t \in T} p_t^{Nloss}, \quad (45)$$

$$R = 1 - \frac{\Delta T_i \left( \sum_{j \in k^{bus}} a_j p_{j,s,t}^{Loss} + \sum_{j \in k^{nd}} b_j h_{j,s,t}^{Loss} \right) + \Delta T_r \left( \sum_{j \in k^{bus}} a_j p_{j,s,t}^{Loss} + \sum_{j \in k^{nd}} b_j h_{j,s,t}^{Loss} \right)}{\Delta T_i \left( \sum_{j \in k^{bus}} a_j + \sum_{j \in k^{nd}} b_j \right) + \Delta T_r \left( \sum_{j \in k^{bus}} a_j + \sum_{j \in k^{nd}} b_j \right)}. \quad (46)$$

## 4. Proposed Distributed Solution for CSRMM

IEHS comprises two entities, i.e., electric and heating systems, which may not be consistently managed by a single central operator [27]. Additionally, the centralized solution method produces extensive information transmission, compromising the information privacy of each entity. Thus, we propose an adaptive ADMM in this section to realize the independent decision-making and highly efficient coordination optimization of IEHS, as shown in Fig 2.

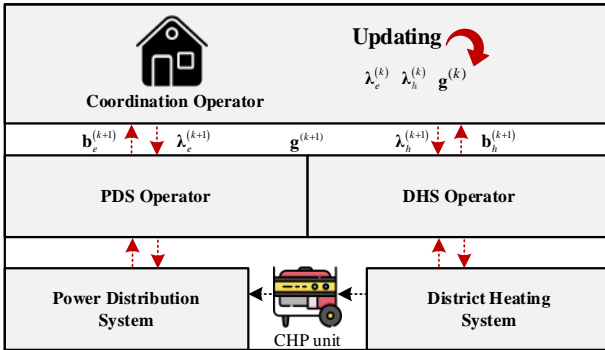


**Fig.2.** Information exchange framework for CSRMM based on ADMM

### 4.1. CSRMM in Compact Form

The multiperiod coordinated restoration problem is expressed in a compact matrix form as

$$\min f \quad (47)$$

$$s.t. \mathbf{I}(\mathbf{x}_e, \mathbf{x}_h, \mathbf{b}) \geq 0, \mathbf{E}(\mathbf{x}_e, \mathbf{x}_h, \mathbf{b}) = 0 \quad (48)$$

where  $f$  denotes the objective function of CSRMM,  $\mathbf{I}(\mathbf{x}_e, \mathbf{x}_h, \mathbf{b}) \geq 0$  and  $\mathbf{E}(\mathbf{x}_e, \mathbf{x}_h, \mathbf{b}) = 0$  are inequality and

equality constraints,  $\mathbf{x}_e$  and  $\mathbf{x}_h$  are local variables in PDS and DHS respectively,  $\mathbf{b}$  is the boundary variables.

### 4.2. Adaptive-ADMM for CSRMM

#### 4.2.1 Decoupling mechanism for CSRMM based on ADMM

As shown in Fig 2, the CSRMM is decomposed into the MISOCP subproblem in PDS and a mixed integer linear programming (MILP) subproblem in DHS. Take the power outputs of CHP units on the connecting line between PDS and DHS as coupling variables in (49) and enable them to satisfy the consistency constraint  $\mathbf{b}_e - \mathbf{b}_h = 0$ .

$$\mathbf{b}_e = \mathbf{p}^{CHP}, \mathbf{b}_h = \mathbf{P}^{CHP}, \quad (49)$$

where  $\mathbf{p}^{CHP}$  and  $\mathbf{P}^{CHP}$  are the vectors indicating the power output of the CHP unit obtained in DHS and PDS.

It is worth noting that the global variables can be used to ensure the consistency of boundary information, which is formulated as follows:

$$\mathbf{g} = \frac{\mathbf{b}_e + \mathbf{b}_h}{2}, \quad (50)$$

#### 4.2.2 PDS subproblem

The penalty terms are added to the objective functions of the PDS subproblems to ensure consistency, which is described as:

$$\min L_e + \lambda_e^{(k)\top} (\mathbf{b}_e^{(k+1)} - \mathbf{g}^{(k)}) + (\rho^{(k)} / 2) \|\mathbf{b}_e^{(k+1)} - \mathbf{g}^{(k)}\|_2^2 \quad (51)$$

$$s.t. \mathbf{I}_e(\mathbf{x}_e, \mathbf{b}_e) \geq 0, \quad \mathbf{E}_e(\mathbf{x}_e, \mathbf{b}_e) = 0, \quad (52)$$

where  $L_e$  includes the electric load loss during fault isolation and restoration stages and the network loss penalty in the objective function of CSRMM,  $\mathbf{I}_e$  and  $\mathbf{E}_e$  are compact representations of inequality and equality constraints of the PDS subproblem,  $\rho^{(k)}$  represents the step size in the  $k^{\text{th}}$  iteration,  $\lambda_e^{(k)}$  represents the Lagrangian multipliers in PDS subproblem. This subproblem is solved by PDS to determine its local variables.

#### 4.2.3 DHS subproblem

The DHS subproblem is represented as follows:

$$\min L_h + \lambda_h^{(k)\top} (\mathbf{b}_h^{(k+1)} - \mathbf{g}^{(k)}) + (\rho^{(k)} / 2) \|\mathbf{b}_h^{(k+1)} - \mathbf{g}^{(k)}\|_2^2 \quad (53)$$

$$s.t. \mathbf{I}_h(\mathbf{x}_h, \mathbf{b}_h) \geq 0, \quad \mathbf{E}_h(\mathbf{x}_h, \mathbf{b}_h) = 0, \quad (54)$$

where  $L_h$  includes the heat load loss during the whole recovery progress in the objective function of CSRMM,  $\mathbf{I}_h$  and  $\mathbf{E}_h$  are compact representations of inequality and equality constraints of the DHS subproblem,  $\lambda_h^{(k)}$  represents the Lagrangian multipliers in DHS subproblem.

#### 4.2.4 Distributed Solution based on Adaptive-ADMM

The power dispatch center and thermal dispatch center respectively control the distribution network and heating

network for local optimization. They transmit the optimized coupling information, i.e., the power outputs of CHP units on the connecting line between PDS and DHS, to the joint dispatch center (JDC). JDC processes the above coupling information to generate the global variables for this iteration and the required Lagrange multipliers for the next iteration using ADMM. The detailed iteration process of the adaptive ADMM is summarized as follows:

Adaptive-ADMM for CSRM	
1	Establish CSRM considering network reconfiguration with SOPs
2	Set the initial values for the global variables, local variables, and Lagrangian multipliers in PDS and DHS
3	<b>for</b> k=1,2,3,...,Max_iter
	PDS solves its subproblem (51)-(52), independently to obtain the power output of the CHP $\mathbf{b}_e^{(k+1)}$ ; DHS solves its subproblem (53)-(54), to obtain the power output of the CHP $\mathbf{b}_h^{(k+1)}$
4	Update global variables $\mathbf{g}^{(k+1)}$ to exchange messages between both sides are optimized separately
5	Determine the variable step size $\rho^{(k+1)}$ in each iteration
6	Calculate the primal and dual convergence residuals
7	<b>if</b> $pr^{(k+1)} < \varepsilon, dr^{(k+1)} < \varepsilon$
8	<b>break</b>
9	<b>else</b>
10	Update Lagrange multipliers $\lambda_e^{(k+1)}, \lambda_h^{(k+1)}$ and skip to step 3 until the ADMM converges
11	<b>end</b>
12	<b>end</b>
13	<b>end</b>

When using ADMM, the global variables, and Lagrangian multipliers are typically updated until convergence is achieved, which is formulated as

$$\mathbf{g}^{(k+1)} = (\mathbf{b}_h^{(k+1)} + \mathbf{b}_e^{(k+1)}) / 2, \quad (55)$$

$$\lambda_e^{(k+1)} = \lambda_e^{(k)} + \rho^{(k)} (\mathbf{x}_e^{(k+1)} - \mathbf{g}^{(k+1)}), \quad (56)$$

$$\lambda_h^{(k+1)} = \lambda_h^{(k)} + \rho^{(k)} (\mathbf{x}_h^{(k+1)} - \mathbf{g}^{(k+1)}), \quad (57)$$

It is noted that the step size in each iteration has a significant impact on the convergence speed of ADMM. When the step size is large, the original residual is much easier to converge than the dual residual. Thus we design an adaptive ADMM to modify the step size according to the relationship between the original and dual residual for achieving the rapid convergence of ADMM, which is described as

$$\rho^{(k+1)} = \begin{cases} \rho^{(k)} (1 + \omega^{incr}), & \text{if } \|pr^{(k)}\| > \mathcal{G} \|dr^{(k)}\|, \\ \rho^{(k)} (1 + \omega^{decr}), & \text{if } \|dr^{(k)}\| > \mathcal{G} \|pr^{(k)}\|, \\ \rho^{(k)}, & \text{otherwise} \end{cases} \quad (58)$$

where  $pr^{(k+1)}$  and  $dr^{(k+1)}$  are the primal and dual residuals. The most common choices are  $\mathcal{G}=10$  and  $\omega^{incr} = \omega^{decr} = 2$  in all iterations [28].

The criteria for determining whether the iteration converges are shown in equations (59) and (60).

$$pr^{(k+1)} = \max \left( \left\| \mathbf{b}_h^{(k+1)} - \mathbf{g}^{(k)} \right\|_2, \left\| \mathbf{b}_e^{(k+1)} - \mathbf{g}^{(k)} \right\|_2 \right) < \varepsilon, \quad (59)$$

$$dr^{(k+1)} = -\rho^{(k)} \left\| \left( \mathbf{g}^{(k+1)} - \mathbf{g}^{(k)} \right) \right\|_2 < \varepsilon. \quad (60)$$

where  $\varepsilon$  is the maximum convergence error allowed in engineering applications. When  $pr^{(k+1)}$  and  $dr^{(k+1)}$  are both smaller than  $\varepsilon$ , the scheduling results are gained. Otherwise, the local variables, global variables, and Lagrangian multipliers are updated until convergence.

## 5. Case Studies

### 5.1. Case Description

As shown in Fig. 3, a modified P33H14 system is utilized to evaluate the effectiveness of the coordinated restoration strategy with SOPs. The reconfigured 33-bus PDS is inspired by the conventional IEEE 33-bus case, and the construction of the 14-node DHS expands upon the 8-node DHS in [29], following the District Heating Network Design Standard (CJJ34-2016) [29]. Three heat stations are installed in DHS, equipping small-scale CHP units. The CHP units act as the primary providers of power and heat in the P33H14 system. Under the normal operation scenario, the tie switches of L2-19, L3-23, L9-10, and L29-30 are normally open and the tie switches of L15-16, and L24-29 are replaced by SOPs in PDS. In DHS, the sectionalizing valves remain closed, while the tie valves of PN2-11, PN3-9, PN8-9, and PN8-12 are left open. The PDS/DHS network topology is verified by operating on/off the switches/valves as necessary.

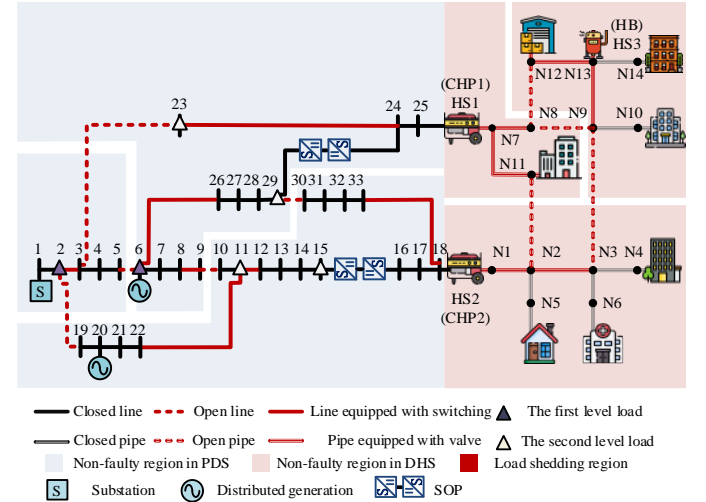


**Fig.3.** Configuration of the modified P33H14 system

The electric and heating loads are 1.29 MW+1.05 MVar and 0.76 MW, respectively. The capacities of the CHP units and DG are 0.5 MW and 0.5 MVA, respectively. The specific parameters are listed in [30]. The experiments are carried out on a computer equipped with an i7-1165G7 CPU and 16 GB of memory, which is programmed by Matlab R2020a.

### 5.2. Restoration effectiveness on modified P33H14 system

This study examines three fault scenarios derived from historical disaster data in Jilin, China, and Barry Island. The scenarios analyzed faults in the DHS, faults in the PDS, and faults in the IEHS, with the affected lines or pipes being randomly generated for each scenario. To assess the impact of

network reconfiguration using SOPs, three cases are carried out:

*Case 1:* the PDS reconfiguration is considered for fault recovery.  
*Case 2:* the SOPs and PDS reconfiguration are combined for restoration.

*Case 3:* the SOPs and coordinated reconfiguration are both considered for load recovery.

### 5.2.1 Analysis of PDS Fault Scenario

In the PDS fault scenario, lines L6-26, L8-9, L11-12, and L23-24 are damaged by disasters. Fig.4 shows the network topologies for service restoration. Table 1 presents the proportion of load recovery at buses/nodes and Table 2 presents total load restoration and resilience metrics. The following are the main conclusions.

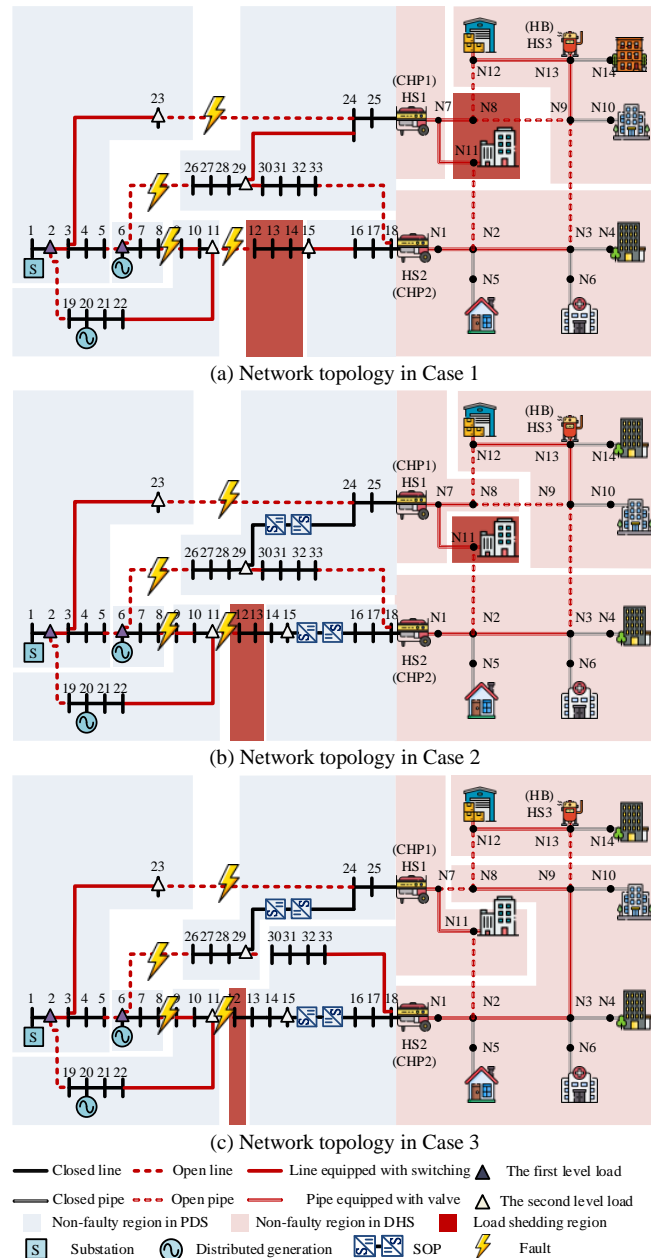


**Fig.4.** Network topology in the service restoration stage

i) The faults arising in the PDS would spread to the DHS

through the CHP units following a disaster, resulting in major energy interruption in DHS. The power production of CHP1 is restricted because of the complete loss of electric load at bus B23 and the partial loss of heat loads at nodes N8, and N11 during the fault isolation stage (shown in Table 1).

ii) SOPs could provide extra power to lost electric loads timely to guarantee longer power supplies during the whole recovery process.

In Case 2, during the fault isolation stage, the SOP of L15-16 provides extra power for the electric load at bus B14. During the service restoration stage, the SOP operation of L24-29 combines with the switch operation of L18-33 and L29-30 for better electric load restoration.

iii) By effectively reorganizing the heating network structure and promoting operational flexibility of coupling units, DHS reconfiguration can offer greater reliability for PDS load restoration.

In Case 3, during the service restoration stage, the lost heat load at N8 is transferred by operating the valves on pipes PN3-9, PN7-8, and PN8-9 to CHP2. The SOP of L15-16 adjusts the power generation of CHP2 to ensure the power supply for electric loads in its island. Then, CHP2 is fully utilized to guarantee the optimal energy supply to connected loads. Only electric loads at bus B12 are partially lost.

iv) Coordinated reconfiguration with SOPs can achieve a better service restoration in PDS. As shown in Table 2, the electric load shedding declines by 46.2%, and the value of  $R$  rises by 20.3% in Case 2 compared with Case 1. The electric load shedding declines by 44.6%, and the value of  $R$  rises by 9.6% in Case 3 compared with Case 2.

**Table 1**  
Proportion of load restoration at buses/nodes

Bus/Node	Isolation Stage		Restoration Stage		
	Case 1	Case 2/Case 3	Case 1	Case 2	Case 3
B12	0%	21%	13%	23%	35%
B14	0%	65%	73%	100%	100%
B23	0%	0%	100%	100%	100%
N8	8%	78%	11%	100%	100%
N11	0%	54%	3%	67%	100%

**Table 2**  
Load loss and resilience metrics

Fault scenario	Case	Total load loss (kW)	Load loss (kW)		Resilience metrics $R$
			Electric	Heat	
PDS fault scenario	Case 1	210	104	106	0.69
	Case 2	83	56	27	0.83
	Case 3	31	31	0	0.91
DHS fault scenario	Case 1	352	118	234	0.60
	Case 2	200	94	106	0.70
	Case 3	131	75	56	0.74
IEHS fault scenario	Case 1	534	202	332	0.56
	Case 2	345	156	189	0.63
	Case 3	274	96	178	0.64

### 5.2.2 Analysis of DHS Fault Scenario

In the DHS fault scenario, pipes PN2-3, PN9-13, and PN12-13 are damaged after the disaster outbreak. Tables 3 and 4 present the proportion of load restoration at buses/nodes and switch/valve operation during the recovery process. The following illustrates the primary conclusions:

i) Significant power outages would occur in PDS as a result of the DHS faults propagating to PDS through the CHP units. During the fault isolation stage, the complete loss of heat loads at N3, N4, and N6 limits the power output of CHP2, resulting in the total loss of electric loads at buses B30, B31, B32, and B33 (shown in Table 2).

ii) SOPs can adjust the energy supply of CHP units to prevent fault propagation from DHS during the fault isolation and restoration stages.

In Case 2, during the fault isolation stage, the SOP of L15-16 adjusts the power generation of CHP2 to supply lost electric loads at buses B30, B31, B32, and B33. During the service restoration stage, the SOP of L24-29 adjusts the power output of CHP1 to match switches of lines L18-33, and L29-30 to restore electric loads lost in the last stage.

iii) By remote tie valve scheduling and load transferring among heat sources, the DHS reconfiguration can improve the ability to resist natural disasters in DHS.

In Case 3, during the service restoration stage, the SOP of L24-29 adjusts the power generation of CHP1 to align with the valve operation on pipes PN3-9, PN8-9, and PN7-8, resulting in improved heat load restoration. Heat loads are completely restored by this method.

iv) In Table 2, the heat load loss declines by 54.7%, and the value of  $R$  rises by 16.7% in Case 2 compared with Case 1. The heat load loss declines by 47.2%, and the value of  $R$  rises by 5.7% in Case 3 compared with Case 2.

**Table 3**

Proportion of load restoration at buses/nodes

Bus/Node	Isolation Stage		Restoration Stage		
	Case 1	Case 2/Case 3	Case 1	Case 2	Case 3
B30	0%	2%	100%	100%	78%
B31	0%	11%	100%	100%	89%
B32	0%	18%	100%	100%	100%
B33	0%	29%	100%	100%	100%
N3	0%	0%	0%	0%	100%
N4	0%	0%	0%	0%	100%
N6	0%	0%	0%	0%	100%
N12	0%	0%	0%	0%	100%

**Table 4**

Switch and valve operation during the recovery process

Line/Pipe	Isolation Stage	Restoration Stage		
		Case 1	Case 2	Case 3
PN3-9	0	0	0	1
PN8-9	0	0	0	1
PN8-12	0	0	0	1
L18-33	1	0	0	1
L29-30	0	1	1	0

### 5.2.3 Analysis of IEHS Fault Scenario

In the IEHS fault scenario, lines L6-26, L9-10, L11-12, L23-

24, and pipes PN2-3, PN9-13, PN12-13 are damaged. Tables 5 and 6 present the proportion of load restoration at buses/nodes and switch/valve operation during the recovery process. The main results are illustrated by the following:

i) During fault recovery, faults in PDS/DHS can spread to the other subsystems through the CHP units, causing significant heat and power disruptions in IEHS simultaneously. Table 1 illustrates the complete lack of electric load at bus 23 and heat loads at nodes N3, N4, and N6 causing simultaneous power and heat outages in the IEHS.

ii) SOP operation could provide extra power to lost electric loads and modify the optimal energy supply of connected coupling units, mitigating fault propagation and reducing total load loss in IEHS.

In Case 2, during fault isolation, the SOPs of lines L24-29 and L15-16 adjust the power generation to supply lost loads caused by fault propagation at the last stage. During the service restoration stage, the SOPs of lines L24-29 and L15-16 modify the power output of both CHP units to match the switches of lines L18-33, and L29-30 for load restoration in both subsystems.

iii) The coordinated reconfiguration can completely furnish the flexibility of time-varying network topology for service restoration by adjusting the DHS network configuration in collaboration with the SOP operation.

In Case 3, during the service restoration stage, the SOP of line L15-16 adjusts the power generation of CHP2 to align with the valve operation on pipes PN3-9, PN8-9, and PN8-12, resulting in improved electric and heat load restoration.

iv) In Table 2, the total load loss declines by 35.4%, and the value of  $R$  rises by 12.5% in Case 2 compared with Case 1. The total load loss declines by 20.6%, and the value of  $R$  rises by 1.6% in Case 3 compared with Case 2.

**Table 5**

Proportion of load restoration at buses/nodes

Bus/Node	Isolation Stage		Restoration Stage		
	Case 1	Case 2/Case 3	Case 1	Case 2	Case 3
B23	0%	0%	100%	100%	100%
N8	8%	78%	11%	100%	100%
N11	0%	54%	3%	67%	100%

**Table 6**

Switch and valve operation during the recovery process

Line/Pipe	Isolation Stage	Restoration Stage		
		Case 1	Case 2	Case 3
PN3-9	0	0	0	1
PN8-9	0	0	0	1
PN8-12	0	0	0	1
L3-23	1	1	1	1
L18-33	1	0	0	1
L29-30	0	1	1	0

### 5.3. Convergence of Adaptive-ADMM

To evaluate the accuracy of the adaptive ADMM, we compare the objective attained by the proposed approach and the centralized method on the modified P33H14 system.

As shown in Table 7, under the PDS Fault Scenario, the objective converges to a consistent value after 25 iterations in

Case 2. Remarkably, the objective error between the centralized method and the adaptive ADMM is 0.15%. In the DHS Fault Scenario, the objective converges to a consistent value after 32 iterations in Case 1, with an objective error of 0.17%. In the IEHS Fault Scenario, the objective converges to a consistent value after 29 iterations in Case 3, with an objective error of 0.09%. Fig. 5 depicts the convergence curves of the primal and dual residuals of the proposed algorithm with a feasibility tolerance of  $10^{-4}$  in Case 2 under the PDS Fault Scenario. Both primal and dual residuals exhibit a decrease in convergence curves, eventually attaining convergence accuracy, thus indicating the effectiveness and precision of the proposed algorithm.

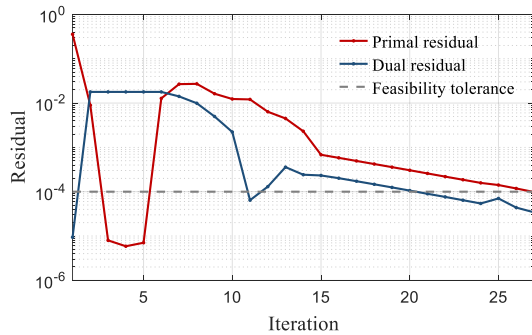


Fig.5. Primal and dual residual versus iteration on P33H14 system.

Table 7  
Load loss and Iteration

Fault scenario	Case	Iteration	Total load loss (kW)	
			Adaptive ADMM	Centralized method
PDS fault scenario	Case 1	35	210	195
	Case 2	25	83	72
	Case 3	54	31	26
DHS fault scenario	Case 1	32	352	301
	Case 2	28	200	168
	Case 3	46	131	113
IEHS fault scenario	Case 1	33	534	490
	Case 2	19	345	310
	Case 3	29	274	251

#### 5.4. Restoration effectiveness on the P118H32 system

The scalability and effectiveness of the coordinated load restoration strategy are tested using an extensive system that consists of a 32-node DHS and a 118-bus PDS, with precise parameters supplied in [30]. Three CHP units, one heating boiler, three distributed generators, and one substation make up the test system. The heating and electric loads are 2.10 MW and 3.11 MW+2.72 MVar respectively. Three cases are conducted to demonstrate the impact of the proposed dispatch strategy on load restoration. Table 8 summarizes the load loss and resilience metrics under three fault scenarios.

When the flexibility of coordinated reconfiguration with SOPs is considered, the load restoration increases. In the IEHS fault scenario, compared with Case 1, the total load restoration in Case 2 is increased by 15.1%. The value of  $R$  has gone up by 6.8%. In Case 3, the overall load restoration has gone up by

9.8% and the value of  $R$  has gone up by 1.3% when compared to the results in Case 2.

Table 8  
Load loss and resilience metrics

Fault scenario	Case	Total load loss (kW)	Load loss (kW)		Resilience metrics $R$
			Electric	Heat	
PDS fault scenario	Case 1	1145	309	836	0.72
	Case 2	775	327	448	0.80
	Case 3	713	247	466	0.86
DHS fault scenario	Case 1	746	522	224	0.81
	Case 2	562	450	112	0.90
	Case 3	125	73	52	0.98
IEHS fault scenario	Case 1	1127	851	276	0.73
	Case 2	957	473	484	0.78
	Case 3	863	439	424	0.79

## 6. Conclusions

In this paper, distributed coordinated reconfiguration with SOPs for resilience-oriented restoration is proposed, which considers the interaction between fault isolation and service restoration stages and emphasizes the complicated coupling characteristics between PDS and DHS. The case studies validate that: i) SOP operation could provide extra power to lost electric loads and modify the optimal energy supply of connected coupling units, mitigating fault propagation and reducing total load loss in IEHS; ii) the DHS network structure is adjusted in collaboration with the PDS switching operation, which can prevent excessive load shedding and halt tremendous fault propagations in respective networks; iii) the adaptive ADMM is proposed to guarantee the privacy of electric and heating systems, which automatically modifies the step size to achieve the rapid convergence of ADMM.

In our future work, we will conduct comprehensive research that considers the disparity in time scales between PDS/DHS in large-scale urban areas. Also, future research will examine integrated reconfiguration with repair for enhancing long-term restoration.

## Acknowledgements

This work was supported by National Natural Science Foundation of China (Grant No. U22A6007, and 52307131).

## References

- [1] Sarantakos I, Zografou-Barredo N-M, Huo D, Greenwood D. A Reliability-Based Method to Quantify the Capacity Value of Soft Open Points in Distribution Networks. *IEEE Trans Power Syst* 2021;36:5032–43.
- [2] Amirioun MH, Aminifar F, Shahidehpour M. Resilience-Promoting Proactive Scheduling Against Hurricanes in Multiple Energy Carrier Microgrids. *IEEE Trans Power Syst* 2019;34:2160–8.
- [3] Darestani YM, Shafieezadeh A, DesRoches R. Effects of Adjacent Spans and Correlated Failure Events on System-Level

- Hurricane Reliability of Power Distribution Lines. *IEEE Trans Power Syst* 2021;36:5032–43.
- [4] Busby JW, Baker K, Bazilian MD, Gilbert AQ, Grubert E, Rai V, et al. Cascading risks: Understanding the 2021 winter blackout in Texas. *Energy Research & Social Science* 2021;77:102106.
- [5] Jiang T, Sun T, Liu G, Li X, Zhang R, Li F. Resilience Evaluation and Enhancement for Island City Integrated Energy Systems. *IEEE Trans Smart Grid* 2022;13:2744–60.
- [6] Liu J, Qin C, Yu Y. Enhancing Distribution System Resilience With Proactive Islanding and RCS-Based Fast Fault Isolation and Service Restoration. *IEEE Trans Smart Grid* 2020;11:2381–95.
- [7] Liu J, Qin C, Yu Y. A Comprehensive Resilience-Oriented FLISR Method for Distribution Systems. *IEEE Trans Smart Grid* 2021;12:2136–52.
- [8] Lei S, Chen C, Song Y, Hou Y. Radiality Constraints for Resilient Reconfiguration of Distribution Systems: Formulation and Application to Microgrid Formation. *IEEE Trans Smart Grid* 2020;11:3944–56.
- [9] Gao H, Chen Y, Xu Y, Liu C-C. Resilience-Oriented Critical Load Restoration Using Microgrids in Distribution Systems. *IEEE Trans Smart Grid* 2016;7:2837–48.
- [10] Yan M, He Y, Shahidehpour M, Ai X, Li Z, Wen J. Coordinated Regional-District Operation of Integrated Energy Systems for Resilience Enhancement in Natural Disasters. *IEEE Trans Smart Grid* 2019;10:4881–92.
- [11] Li G, Yan K, Zhang R, Jiang T, Li X, Chen H. Resilience-Oriented Distributed Load Restoration Method for Integrated Power Distribution and Natural Gas Systems. *IEEE Trans Sustain Energy* 2022;13:341–52.
- [12] Lin Y, Chen B, Wang J, Bie Z. A Combined Repair Crew Dispatch Problem for Resilient Electric and Natural Gas System Considering Reconfiguration and DG Islanding. *IEEE Trans Power Syst* 2019;34:2755–67.
- [13] “Flexibility Improvement of Power Systems: Technical Paths, Economies, and Policy Recommendations” [Online]. Available: <http://www.nrdc.cn/Public/uploads/2022-07-18/62d4c2e313df1.pdf>
- [14] Pan Z, Guo Q, Sun H. Feasible region method based integrated heat and electricity dispatch considering building thermal inertia. *Appl Energy* 2017;192:395–407.
- [15] Khatibi M, Bendtsen JD, Stoustrup J, Molbak T. Exploiting Power-to-Heat Assets in District Heating Networks to Regulate Electric Power Network. *IEEE Trans Smart Grid* 2021;12:2048–59.
- [16] Ding Y, Shao C, Hu B, Bao M, Niu T, Xie K, et al. Operational Reliability Assessment of Integrated Heat and Electricity Systems Considering the Load Uncertainties. *IEEE Trans Smart Grid* 2021;12:3928–39.
- [17] Sarantakos I, Zografou-Barredo N-M, Huo D, Greenwood D. A Reliability-Based Method to Quantify the Capacity Value of
- Soft Open Points in Distribution Networks. *IEEE Trans Power Syst* 2021;36:5032–43.
- [18] Mao D, Wang P, Wang W, Ni L. Reliability segment design in single-source district heating networks based on valve network models. *Sustainable Cities and Society* 2020;63:102463.
- [19] Chen F, Chen Y, Deng H, Lin W, Shao Z. Distributed robust operation of integrated energy system considering gas inertia and biogas–wind renewables. *Int J Electr Power Energy Syst* 2023;151:109123.
- [20] Chen F, Deng H, Chen Y, Wang J, Jiang C, Shao Z. Distributed robust cooperative scheduling of multi-region integrated energy system considering dynamic characteristics of networks. *Int J Electr Power Energy Syst* 2023;145:108605.
- [21] Cao W, Wu J, Jenkins N, Wang C, Green T. Operating principle of Soft Open Points for electrical distribution network operation. *Appl Energy* 2016;164:245–57.
- [22] Zhang T, Mu Y, Dong L, Jia H, Pu T, Wang X. Fully parallel decentralized load restoration in coupled transmission and distribution system with soft open points. *Appl Energy* 2023;349:121626.
- [23] Lv C, Liang R, Jin W, Chai Y, Yang T. Multi-stage resilience scheduling of electricity-gas integrated energy system with multi-level decentralized reserve. *Appl Energy* 2022;317:119165.
- [24] Yao S., Gu W., Lu S., Zhou S., Wu Z., Pan G., He D., “Dynamic Optimal Energy Flow in the Heat and Electricity Integrated Energy System,” *IEEE Trans. Sustain. Energy*, 2021;12:179–190.
- [25] Aghaei J, Agelidis VG, Charwand M, Raeisi F, Ahmadi A, Nezhad AE, et al. Optimal Robust Unit Commitment of CHP Plants in Electricity Markets Using Information Gap Decision Theory. *IEEE Trans Smart Grid* 2017;8:2296–304.
- [26] Massrur HR, Niknam T, Aghaei J, Shafie-khah M, Catalao JPS. Fast Decomposed Energy Flow in Large-Scale Integrated Electricity–Gas–Heat Energy Systems. *IEEE Trans Sustain Energy* 2018;9:1565–77.
- [27] Yang W., Liu W., Chung C. Y., and Wen F., “Coordinated planning strategy for integrated energy systems in a district energy sector,” *IEEE Trans Sustain Energy*, 2020;11:1807–1819.
- [28] S. Boyd, N. Parikh, E. Chu, B. Peleato, and J. Eckstein, “Distributed optimization and statistical learning via the alternating direction method and multipliers,” *Found. Trends Mach. Learn.*, 2011;3,1–122.
- [29] Wang K, Xue Y, Guo Q, Shahidehpour M, Zhou Q, Wang B, et al. A Coordinated Reconfiguration Strategy for Multi-Stage Resilience Enhancement in Integrated Power Distribution and Heating Networks. *IEEE Trans Smart Grid* 2023;14:2709–22.
- [30] “Test data in Matlab format”, 2023. [Online]. Available: <https://docs.google.com/spreadsheets/d/1tIDi9qdoc0xzCRZd4DRZiazImKiUhJ5a/edit?usp=sharing&oid=105955957003523749518&rtopof=true&sd=true>